A Rule of Thumb for the Detectability of Gravitational-Wave Bursts

Patrick J. Sutton

School of Physics and Astronomy, Cardiff University, Cardiff, United Kingdom, CF24 3AA

E-mail: patrick.sutton@astro.cf.ac.uk

Abstract. We derive a simple relationship between the energy emitted in gravitational waves for a narrowband source and the distance to which that emission can be detected by a single detector. We consider linearly polarized, elliptically polarized, and unpolarized gravitational waves, and emission patterns appropriate for each of these cases. We ignore cosmological effects.

PACS numbers: 04.80.Nn

1. Introduction

The sensitivity of a gravitational-wave detector to a transient signal ("burst") is reasonably well characterised by the expectation value of the matched-filter signal-to-noise ratio (SNR) of the burst [1]. This expectation value can be computed as an integral of the burst signal spectrum divided by the detector noise spectral density. For the most commonly considered gravitational-wave transient signals, the inspiral of neutron star binaries, this leads to the well-known average (or "sensemon"‡) range [2] giving the effective volume within which the expected SNR in a single detector would be above some threshold $\rho_{\rm det}$:

$$\mathcal{R}_{\rm BNS} = 1.77 \left(\frac{5\mathcal{M}^{5/3} f_{7/3}}{96\pi^{4/3}\rho_{\rm det}^2} \right)^{1/2} . \tag{1}$$

Here $\mathcal{M}$ is the chirp mass of the binary and $f_{7/3} = \int df\, f^{-7/3} S^{-1}$ where S is the noise power spectrum of the detector. The factor 1.77 arises from integration over possible positions and orientations of the binary. The average range $\mathcal{R}_{\rm BNS}$ is defined such that for a homogenous isotropic distribution of sources with rate density $\dot{\mathcal{N}}$ the mean rate of detections will then be

$$\dot{N} = \frac{4}{3}\pi (\mathcal{R}_{\rm BNS})^3 \dot{\mathcal{N}} . \tag{2}$$

‡ The other commonly used range for inspirals is the "horizon" range, defined as the maximum distance at which an optimally positioned and oriented binary would produce an expected SNR of at least $\rho_{\rm det}$. The horizon range is a factor 2.26 larger than the average range.

The average range is clearly a useful tool for assessing the scientific capabilities of a detector. Unfortunately, while the expected gravitational-wave emission of binary systems is well-understood, gravitational wave transients from most other potential sources such as supernovae, long gamma-ray bursts, and soft gamma repeaters are not known reliably. In this technical note we present a simple definition of the effective sensitive range of a gravitational-wave detector to generic bursts, based on the total energy emitted in the burst and the peak frequency of the emission. This range is appropriate for a variety of possible signal polarizations and source emission patterns, and requires only that the signal bandwidth is smaller than the frequency range over which the detector noise spectrum varies significantly.

We begin by determining how the total energy $E_{\rm GW}$ carried in a gravitational-wave burst is related to the measure of signal strength commonly used in burst searches, the root-sum-square amplitude $h_{\rm rss}$. We then relate these measures to the expected signal-to-noise ratio ρ, and define an average range analogous to equation (1). Finally, we compare this range to the results of recent LIGO-Virgo searches for gravitational-wave bursts [3, 4, 5].

2. Relating $E_{\rm GW}$ to $h_{\rm rss}$

We first relate the total energy emitted in gravitational waves, $E_{\rm GW}$, to the LIGO-Virgo standard measure for burst amplitude at the detector, $h_{\rm rss}$. The latter is defined by

$$h_{\rm rss} = \int_{-\infty}^{\infty} dt \, \left[h_+^2(t) + h_\times^2(t)\right] \tag{3}$$

$$= 2\int_0^{\infty} df \, \left[|\tilde{h}_+(f)|^2 + |\tilde{h}_\times(f)|^2\right] . \tag{4}$$

The flux (energy per unit area per unit time) of a gravitational wave is

$$F_{\rm GW} = \frac{c^3}{16\pi G}\langle \dot{h}_+^2(t) + \dot{h}_\times^2(t)\rangle \, , \tag{5}$$

where the angle brackets denote an average over several periods. For a burst of duration $\leq T$ we can compute the average by integrating over the duration:

$$F_{\rm GW} = \frac{c^3}{16\pi G}\frac{1}{T}\int_{-T/2}^{T/2} dt \, \left[\dot{h}_+^2(t) + \dot{h}_\times^2(t)\right] \tag{6}$$

$$= \frac{c^3}{16\pi G}\frac{1}{T}\int_{-T/2}^{T/2} dt \, \left[\int_{-\infty}^{\infty} df' e^{i2\pi f' t}(i2\pi f')\tilde{h}_+^*(f') \int_{-\infty}^{\infty} df e^{-i2\pi f t}(-i2\pi f)\tilde{h}_+(f) + (\text{same}, + \to \times)\right] \tag{7}$$

Since $h_{+,\times} \to 0$ outside $-T/2 < t < T/2$, we may extend the time integration to $t \to \pm\infty$. The time integral then evaluates to a delta function, $\delta(f - f')$, giving

$$F_{\rm GW} = \frac{\pi c^3}{4G}\frac{1}{T}\int_{-\infty}^{\infty} df f^2 \left(|\tilde{h}_+(f)|^2 + |\tilde{h}_\times(f)|^2\right) . \tag{8}$$

2.1. Isotropic emission

To compute the total energy $E_{\rm GW}$ emitted, we need to integrate the flux $F_{\rm GW}$ assuming some emission pattern. Let us first assume isotropic emission. Then for a source at a distance r

$$E_{\rm GW} = 4\pi r^2\, T F_{\rm GW} \tag{9}$$

$$= \frac{\pi^2 c^3}{G} r^2 \int_{-\infty}^{\infty} df\, f^2 \left(|\tilde{h}_+(f)|^2 + |\tilde{h}_\times(f)|^2 \right) . \tag{10}$$

If we assume that the signal is narrowband with central frequency f_0, we obtain

$$E_{\rm GW} = \frac{\pi^2 c^3}{G} r^2 f_0^2 h_{\rm rss}^2 \, . \tag{11}$$

2.2. Linear motion emission

Axisymmetric motion will produce linearly polarized emission with pattern

$$h_+(t) = \sin^2(\iota)\, h(t) \, , \tag{12}$$

$$h_\times(t) = 0 \, , \tag{13}$$

where ι is the angle between the symmetry axis and the line-of-sight to the observer, and we have selected a polarization basis aligned with this symmetry axis. The energy emitted in a narrowband signal is then

$$E_{\rm GW} = \frac{\pi c^3}{4G} r^2 \int_{-1}^{1} d(\cos\iota) \int_0^{2\pi} d\lambda \int_{-\infty}^{\infty} df\, f^2 \left(\sin^4(\iota)\, |\tilde{h}(f)|^2 \right)$$

$$= \frac{8}{15} \frac{\pi^2 c^3}{G} r^2 f_0^2 h_{\rm rss}^2 \, , \tag{14}$$

where λ is the azimuthal angle in the source frame. This is 8/15 times the result for isotropic emission, (11).

Note that in writing (14) we have defined $h_{\rm rss}$ as the root-sum-square amplitude from an *optimally oriented* source ($\iota = \pi/2$ in this case). This differs slightly from the standard LIGO-Virgo definition, which includes the inclination factors. In practice, however, LIGO-Virgo papers to date have typically simulated optimally oriented sources.

2.3. Rotating system emission

Rotational motion (such as from a circular binary) will produce emission with pattern

$$h_+(t) = \frac{1}{2}(1 + \cos^2(\iota))\, A(t) \cos\Phi(t) \, , \tag{15}$$

$$h_\times(t) = \cos(\iota)\, A(t) \sin\Phi(t) \, , \tag{16}$$

where ι is the angle between the rotation axis and the line-of-sight to the observer, and we have again selected a polarization basis aligned with this symmetry axis. We assume $A(t)$ varies slowly enough compared to $\Phi(t)$ that h_+ and $h_\times$ are approximately

orthogonal. This produces an elliptically polarized signal at the detector. The energy emitted in a narrowband signal is

$$\begin{aligned} E_{\rm GW} &= \frac{\pi c^3}{4G} r^2 \int_{-1}^{1} d(\cos\iota) \int_0^{2\pi} d\lambda \int_{-\infty}^{\infty} df\, f^2 \left(\frac{(1+\cos^2(\iota))^2}{4} + \cos^2(\iota) \right) |\tilde{h}(f)|^2 \\ &= \frac{2}{5} \frac{\pi^2 c^3}{G} r^2 f_0^2 h_{\rm rss}^2 \,, \end{aligned} \tag{17}$$

where $\tilde{h}(f)$ is the Fourier transform of $A(t)\cos\Phi(t)$ and we have again used $h_{\rm rss}$ for an optimally oriented source ($\iota = 0$). The expression for energy emitted is 2/5 times the result for isotropic emission, (11).

3. Relating $E_{\rm GW}$ to Signal-To-Noise Ratio

The detectability of a generic signal is determined mainly by its expected signal-to-noise ratio ρ for a matched filter. (The time-frequency volume $V_{\rm TF}$ of the signal is also important when $V_{\rm TF} \gg 1$ [1, 6]). For a narrowband signal, ρ has a simple relationship to the $h_{\rm rss}$ amplitude. We start from

$$\rho^2 = 2 \int_{-\infty}^{\infty} \frac{df}{S(f)} \frac{|F_+ \tilde{h}_+(f) + F_\times \tilde{h}_\times(f)|^2}{S(f)} \,, \tag{18}$$

where $S(f)$ is the one-sided noise power spectrum, and $F_{+,\times}(\theta,\phi,\psi)$ are the antenna responses to the sky position (θ,ϕ) and polarization ψ of the gravitational wave. We may expand the square in (18) and drop the $\tilde{h}_+ \tilde{h}_\times^*$ terms for most signals of interest: for elliptically polarized signals the two waveforms are orthogonal, while for linearly polarized signals $\tilde{h}_\times = 0$. The waveforms are also orthogonal in the *unpolarized* case, where the two polarizations are independent stochastic timeseries. An example is white-noise bursts [5]. Assuming a narrowband signal, we find

$$\rho^2 = \Theta^2 \frac{h_{\rm rss}^2}{S(f_0)} \,, \tag{19}$$

where we define the angle factor

$$\Theta^2 \equiv \begin{cases} F_+^2(\theta,\phi,\psi) + F_\times^2(\theta,\phi,\psi) & \text{isotropic unpolarized} \\ F_+^2(\theta,\phi,\psi)(\frac{1+\cos^2(\iota)}{2})^2 + F_\times^2(\theta,\phi,\psi)\cos^2(\iota) & \text{elliptical} \\ F_+^2(\theta,\phi,\psi)\, 2\sin^4\iota & \text{linear} \end{cases} \tag{20}$$

Note that all dependence on the four angles θ, ϕ, ψ, and ι is contained in Θ. Substituting (11), (14), or (17) gives

$$\rho^2 = \frac{\Theta^2}{\alpha} \frac{G}{\pi^2 c^3} \frac{E_{\rm GW}}{S(f_0) r^2 f_0^2} \,, \tag{21}$$

where $\alpha = 1$ for isotropic emission, 8/15 for linearly polarized emission, and 2/5 for circularly polarized emission.

4. Effective Range

We can now combine the results for $E_{\rm GW}$ and ρ to compute the typical distance to which a source is detectable. We will follow the approach used in Section V of [2].

Consider a homogenous isotropic distribution of sources with rate density $\dot{\mathcal{N}}$. A signal from a given source will be detectable if the received signal-to-noise is above some threshold value $\rho_{\rm det}$. The mean rate of detections will then be

$$\dot{N} = 4\pi\dot{\mathcal{N}}\int_0^\infty dr r^2 P(\rho^2 > \rho_{\rm det}^2)\,. \tag{22}$$

Here $P(\rho^2 > \rho_{\rm det}^2)$ is the probability that the signal-to-noise of a source at given distance r with random θ, ϕ, ψ, and ι will be above threshold. Using (21), we may write this probability as

$$P(\rho^2 > \rho_{\rm det}^2) = P(\Theta^2 > r^2/r_0^2)\,, \tag{23}$$

where we have defined the fiducial distance

$$r_0^2 = \frac{G}{\alpha\pi^2 c^3}\frac{E_{\rm GW}}{S(f_0)f_0^2\rho_{\rm det}^2}\,. \tag{24}$$

Our detection rate is thus

$$\dot{N}_{\rm det} = \frac{4}{3}\pi r_0^3\dot{N}\left[3\int_0^\infty dx\, x^2 P(\Theta^2 > x^2)\right]\,. \tag{25}$$

The integral is easily evaluated numerically:

$$\int_0^\infty dx\, x^2 P(\Theta^2 > x^2) = \begin{cases} 0.0978 & \text{unpolarized} \\ 0.0287 & \text{elliptical} \\ 0.0537 & \text{linear} \end{cases} \tag{26}$$

Following [2], we define the effective detection range $\mathcal{R}_{\rm eff}$ as the radius enclosing a spherical volume V such that the rate of detections is $\dot{\mathcal{N}}V$:

$$\mathcal{R}_{\rm eff} = r_0\left[3\int_0^\infty dx\, x^2 P(\Theta^2 > x^2)\right]^{1/3} \tag{27}$$

$$= \beta\left(\frac{G}{\pi^2 c^3}\frac{E_{\rm GW}}{S(f_0)f_0^2\rho_{\rm det}^2}\right)^{1/2}\,, \tag{28}$$

where

$$\beta \equiv \alpha^{-1/2}\left[3\int_0^\infty dx\, x^2 P(\Theta^2 > x^2)\right]^{1/3} = \begin{cases} 0.665 & \text{unpolarized} \\ 0.698 & \text{elliptical} \\ 0.745 & \text{linear} \end{cases}\,. \tag{29}$$

We note that for all three cases (unpolarized, linear, and elliptical polarizations), β is equal to $1/\sqrt{2}$ to within a few percent. A convenient approximation is thus

$$\mathcal{R}_{\rm eff} \simeq \left(\frac{G}{2\pi^2 c^3}\frac{E_{\rm GW}}{S(f_0)f_0^2\rho_{\rm det}^2}\right)^{1/2}\,. \tag{30}$$

With this definition the mean rate of detections for a homogenous isotropic distribution of standard-candle (fixed $E_{\rm GW}, f_0$) burst sources with rate density $\dot{\mathcal{N}}$ is

$$\dot{N} = \frac{4}{3}\pi(\mathcal{R}_{\rm eff})^3\dot{\mathcal{N}}\,. \tag{31}$$

5. Example: LIGO-Virgo Science Runs, 2005–2010

As an example, we apply our effective range formula (30) to the LIGO-Virgo network during their 2005–07 and 2009–10 science runs. The results of the search for generic gravitational-wave bursts are reported in [3, 4, 5]. Approximately 1.8 yr of coincident data were analysed from the three LIGO detectors (H1, H2, L1) and the Virgo detector (V1). No gravitational waves were detected, and limits were placed on the rate, amplitude, and energy content of gravitational waves.

Figure 1(a) shows an example noise spectrum from each of the detectors that participated in the 2009-10 run (data obtained from [7]). The H1 detector had the lowest noise level across most of the search frequency band, so for convenience we use its noise spectrum $S(f)$ for our range calculations. The other quantity required for defining the range is the SNR threshold $\rho_{\rm det}$, which is the threshold at which the detection efficiency is 50%. Comparing the $h_{\rm rss}$ amplitude limits for linearly polarized sine-Gaussian bursts and unpolarized white-noise bursts (Tables II and IV of [5], Table II of [4], Fig. 3 of [3]) show that they correspond to $\rho_{\rm det} \simeq 20$ to 30 as measured against the H1 S6 noise spectrum§, depending on the waveform, network, and data set. Since we expect the rate limits to be dominated by the most sensitive data (due to volume scaling), we select $\rho_{\rm det} = 20$ for our estimates.

Figure 1(b) shows the effective range (30) predicted assuming $\rho_{\rm det} = 20$ and the H1 noise curve smoothed to 10 Hz resolution. The left-hand scale (Mpc) assumes $E_{\rm GW} = 10^{-2} M_\odot c^2$, which is the approximate maximum gravitational-wave emission possible from long gamma-ray bursts under the most optimistic scenarios [8, 9, 10, 11, 12, 13, 14]. The right-hand scale (kpc) assumes $E_{\rm GW} = 10^{-8} M_\odot c^2$, which is a typical energy emission in simulations of core-collapse supernovae [15, 16]. The maximum ranges in the two cases are approximately 10 Mpc (10 kpc) for signal frequencies around 100 Hz – 200 Hz, dropping to below 1 Mpc (1 kpc) by 1000 Hz.

Figure 1(c) shows the $E_{\rm GW}$ predicted by (30) to be required for a source at a fixed distance of 10 kpc to produce an expected SNR equal to $\rho_{\rm det} = 20$. The dots are the actual $E_{\rm GW}$ values for a variety of waveforms and the 2009–10 H1L1V1 network, as reported in Fig. 7 of [5]. Figure 1(d) shows the 90% confidence rate density limit (rate per unit volume) predicted by (31) for a homogeneous isotropic distribution of standard-candle sources with $E_{\rm GW} = 1 M_\odot c^2$, assuming no detections in the 2005–07 and 2009–10 searches (so that $\dot{N} \leq 2.3$ at 90% confidence). The dots are the approximate rate density limits for linearly polarized sine-Gaussian waveforms set by the combined 2005–07 and 2009–10 data sets (Fig. 6 of [5]). Despite the fact that we use a single sample noise spectrum and SNR threshold to represent all networks and both science runs, the predicted limits are a reasonably good match to the measured limits in each case.

§ The SNR threshold $\rho_{\rm det}$ can be estimated from the amplitude limit $h_{\rm rss}^{50\%}$ using (19, 20): $\rho_{\rm det} \simeq \Theta_{\rm rms} h_{\rm rss}^{50\%} / \sqrt{S(f_0)}$ where $\Theta_{\rm rms} = (\langle F_+^2 + F_\times^2 \rangle_{\theta,\phi,\psi})^{1/2} = \sqrt{2/5}$ for optimally oriented sources.

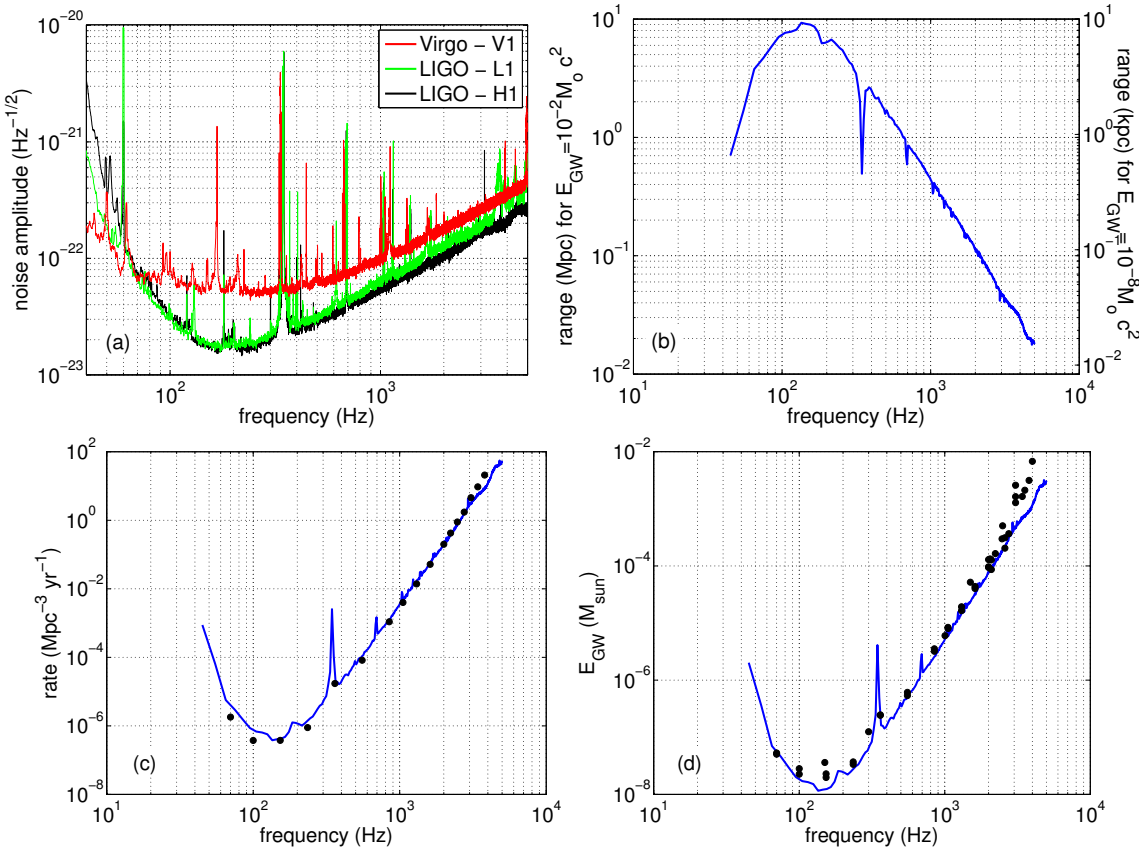

Figure 1. (a) Example noise spectrum from each of the detectors in the 2009–10 LIGO-Virgo science run. (b) Effective range predicted by (30) using $\rho_{\rm det} = 20$ and the H1 noise curve smoothed to 10 Hz resolution. The left-hand (right-hand) scales assume $E_{\rm GW} = 10^{-2} M_\odot c^2$ ($10^{-8} M_\odot c^2$). (c) $E_{\rm GW}$ predicted by (30) to be required for a source at a fixed distance of 10 kpc to produce an expected SNR equal to $\rho_{\rm det} = 20$. The dots are the actual $E_{\rm GW}$ values for a variety of waveforms and the 2009–10 H1L1V1 network [5]. (d) 90% confidence rate density limits predicted by (31) for a homogeneous isotropic distribution of standard-candle sources with $E_{\rm GW} = 1 M_\odot c^2$. The dots are rate density limits for linearly polarized sine-Gaussian waveforms set by the combined 2005–07 and 2009–10 data sets [5].

Acknowledgements

The author would like to thank Eric Chassande-Mottin for motivating this investigation, and for his careful reading of and helpful suggestions on a previous draft. This work was supported in part by STFC grants PP/F001096/1 and ST/J000345/1. This draft has been assigned LIGO document number LIGO-P1000041-v3.

References

[1] W. G. Anderson, P. R. Brady, J. D. E. Creighton, and É. É. Flanagan. Excess power statistic for detection of burst sources of gravitational radiation. *Phys. Rev. D*, 63:042003, 2001.

[2] Lee Samuel Finn and David F. Chernoff. Observing binary inspiral in gravitational radiation: One interferometer. *Phys. Rev. D*, 47(6):2198–2219, Mar 1993.

[3] B. P. Abbott et al. Search for gravitational-wave bursts in the first year of the fifth LIGO science run. *Phys. Rev. D*, 80(10):102001, November 2009.

[4] J. Abadie et al. All-sky search for gravitational-wave bursts in the first joint LIGO-GEO-Virgo run. *Phys. Rev. D*, 81(10):102001, May 2010.

[5] J. Abadie et al. All-sky search for gravitational-wave bursts in the second joint LIGO-Virgo run. *Phys. Rev. D*, 85(12):122007, June 2012.

[6] P. J. Sutton, G. Jones, S. Chatterji, P. Kalmus, I. Leonor, S. Poprocki, J. Rollins, A. Searle, L. Stein, M. Tinto, and M. Was. X-Pipeline: an analysis package for autonomous gravitational-wave burst searches. *New Journal of Physics*, 12(5):053034, May 2010.

[7] J. Abadie et al. All-sky search for gravitational-wave bursts in the second joint LIGO-Virgo run. Technical Report LIGO-P1100118-v24, LIGO Scientific Collaboration, Virgo Collaboration, 2012. `https://dcc.ligo.org/LIGO-P1100118-v24/public`.

[8] M. B. Davies, A. King, S. Rosswog, and G. Wynn. Gamma-Ray Bursts, Supernova Kicks, and Gravitational Radiation. *Astrophysical Journal*, 579:L63–L66, November 2002.

[9] C. L. Fryer, D. E. Holz, and S. A. Hughes. *Astrophys. J.*, 565:430, 2002.

[10] Shiho Kobayashi and Peter Meszaros. Polarized gravitational waves from gamma-ray bursts. *Astrophys. J.*, 585:L89, 2003.

[11] M. Shibata, K. Shigeyuki, and E. Yoshiharu. Dynamical bar-mode instability of differentially rotating stars: effects of equations of state and velocity profiles. *Mon. Not. R. Astron. Soc.*, 343:619, 2003.

[12] Anthony L. Piro and Eric Pfahl. Fragmentation of Collapsar Disks and the Production of Gravitational Waves. *Astrophys. J.*, 658:1173–1176, April 2007.

[13] A. Corsi and P. Meszaros. GRB afterglow plateaus and gravitational waves: Multi-messenger signature of a millisecond magnetar? *Astrophys. J.*, 702:1171, 2009.

[14] G. E. Romero, M. M. Reynoso, and H. R. Christiansen. Gravitational radiation from precessing accretion disks in gamma-ray bursts. *Astron. Astrophys.*, 524:A4, 2010.

[15] Christian D. Ott. The gravitational-wave signature of core-collapse supernovae. *Class. Quantum Grav.*, 26(6):063001, March 2009.

[16] K. Kotake. Multiple physical elements to determine the gravitational-wave signatures of core-collapse supernovae. `http://arxiv.org/abs/1110.5107`.